A multi-stage methodology for wind park inter-array cabling: graph preparation, layout, and sizing

Response to Reviews

This document contains the response to the paper's reviewers ***A multi-stage methodology for wind park inter-array cabling: graph preparation, layout, and sizing***. The authors thank the reviewers and editor for their valuable suggestions. Each comment, suggestion, or recommendation was analysed in detail and answered in the context of the proposed paper. All changes in the paper were highlighted in blue and referenced in this response as a text box.

Editor:

Authors' comment

Editor's Concern 0.1
Dear authors, please use the reviewers' comments as an opportunity to improve the paper. While recognising the general merits of the paper, the comments highlight several important points for improvement.

Authors' response 0.1
We thank the Editor and reviewers for their constructive comments and have carefully considered all points raised; the manuscript has been revised accordingly to address the concerns and improve its clarity and presentation.

1 Reviewer 1

Reviewer's Concern 1.1
The submitted manuscript addresses an interesting and relevant problem: Optimization of inter-array cabling in wind farms. The chosen method, mixed integer linear programming (MILP) is standard.

Authors' response 1.1
For the second and third steps, mixed-integer linear programming (MILP) is widely used as demonstrated in prior studies (Pillai et al., 2015; Wedzik et al., 2016; Fischetti and Pisinger, 2018a, 2018b; Ulku and Alabas-Uslu, 2020; Pérez-Rúa et al., 2020; Souza de Alencar et al., 2025). However, in most of these works, the MILP formulation does not explicitly account for radial array structures and typically introduces two binary variables per arc (one per direction). In contrast, our formulation employs a single binary variable per arc, while allowing the associated flow variable to take both positive and negative values.

Reviewer's Concern 1.2
It is hard to find contributions to the existing literature. Section 1 gives a brief overview of the literature in the field, but fails to identify any research gaps that the submissions claims to close successfully. Neither the 'graph preparation' (Section 2), the model that 'minimises the connections' (Section 3), the model that optimizes the selection of cable types (Section 4), the heuristic that addresses the computational challenge of the model integrating all features (Section 5), represent scientific novelty beyond decent engineering approaches.

Authors' response 1.2
Regarding the general and specific comments, the paper presents a multi-stage methodology addressing three key steps in the optimisation of wind farm array layouts. In the existing literature (Fischetti and Pisinger 2018a,2018b; Pérez-Rúa et al. 2020; Souza de Alencar et al., 2025), it is standard practice to approximate cable lengths using two-dimensional distances between turbines. In contrast, regading the graph preparation from Section 2, we propose a process that incorporates three-dimensional terrain distances. The process accounts for inclination thresholds, includes both hard and soft exclusion zones. Soft exclusion zones, for instance, may represent varying terrain types with distinct trenching costs, which are explicitly considered during pathfinding. This results in a more representative graph for the interconnection optimisation problem.

Regarding routing model in section 3, as presented in our earlier conference paper (Torque), referenced in the introduction, this approach reduces the number of variables compared to recent MILP formulations such as Souza de Alencar et al. (2025), for which a benchmark comparison is provided. This benchmark is not included in the present manuscript, as the conference paper focuses solely on layout optimisation, where benchmarking is directly applicable.

Whereas the current work extends the framework to include conductor size selection and its interaction with the layout process. The conference paper has been accepted and defended in the conference. Now the paper has been published and can be read at https://iopscience.iop.org/article/10.1088/1742-6596/3224/5/052005

Regarding Section 4 and 5, in the third step, the conductor size selection (CSS) process is typically treated in the literature as a post-processing task. In this work, we instead present CSS either in a unified framework with the layout optimisation or as a sequential but integrated step.

This allows CSS to play an active role in the layout decision-making process. For example, the user may define a set of candidate conductor sizes (e.g. ten options) and restrict the final selection to a subset (e.g. three). Treating CSS purely as post-processing can limit optimality, as the shortest connection is not necessarily the most cost-effective, as demonstrated in our case studies. We are currently revising the introduction to more clearly highlight these contributions. In the following bullet points after outlining out the literature criteria;

To address these criteria, the main contributions of this work are as follows:

- A graph construction methodology that incorporates three-dimensional terrain, inclination constraints, and both hard and soft exclusion zones into the candidate edge generation process.
- A reduced MILP formulation for inter-array routing using a single binary variable per arc, thereby decreasing the number of decision variables relative to standard formulations.
- A joint treatment of routing and conductor size selection, allowing CSS to influence layout decisions rather than being treated as post-processing.
- The development and comparison of integrated and sequential approaches for joint routing and CSS, highlighting trade-offs between solution quality and computational complexity.

Reviewer's Concern 1.3

1. The writing quality is not up to the standards of a scientific journal, especially in the more mathematical sections. Nearly none of the mathematical formulas are smoothly integrated with the flow of text, as exemplified already in (1): The trivial statement that $p_i = 1$ for all $i \in \mathcal{N}_t$ is given as a displayed equation separated by two periods, and given a forward reference in the text. Such forward references, where the formula id occurs earlier than the formula itself occur throughout the manuscript, whereas they should be totally avoided.

Authors' response 1.3

We acknowledge the concerns regarding writing quality and the integration of mathematical expressions. We revised the manuscript to improve the flow of the text, ensure proper placement of equations, and eliminate forward references to equations that have not yet been introduced.

3.1 Core formulation

The graph nodes ($\mathcal{N}_{ac}$) are initially partitioned into two sets: turbine nodes $\mathcal{N}_t \subseteq \mathcal{N}_{ac}$ and substation nodes $\mathcal{N}_s \subseteq \mathcal{N}_{ac}$, such that $\mathcal{N}_{ac} = \mathcal{N}_t \cup \mathcal{N}_s$. To maintain power flow tracking within the system, each turbine node injects one unit of power, modelled as a fixed parameter such that $p_i = 1$ for all $i \in \mathcal{N}_t$.

For substation nodes, the net injection is modelled as an integer decision variable representing representing power withdrawal, such that $p_i \in \mathbb{Z}_{\leq 0}$ for all $i \in \mathcal{N}_s$.

Power balance is enforced by requiring that the total substation withdrawal matches the total

turbine injection:

$$\sum_{i \in \mathcal{N}_s} p_i = -|\mathcal{N}_t|. \tag{1}$$

Reviewer's Concern 1.4

2. Several symbols are not carefully introduced before they are used (see a_{ik} in (4)), whereas others are introduced more than once (see the calligraphic letter that probably is an 'M' introduced on lines 167 and 196). Other symbols that are not defined include $S_{a,\iota_{ik}}$ (see (16a)), θ_i and θ_k (see (19)), γ_t, t_i, and s_i (see (20)), etc. Also, while the authors should be perfectly free to choose their own notational style, it is likely that more readers than this reviewer would appreciate less excessive use of calligraphic letters (what do we call the symbol denoting the 'maximum number of string connections' on line 175?)

Authors' response 1.4

We agree that several symbols were not adequately introduced and that some notation was defined more than once. We revided the manuscript to ensure that all symbols are clearly and consistently defined prior to use. For example, for candidate edges we defined $a_{ik} = (i, k)$. We also acknowledge the duplicate definition of $\mathfrak{M}$ (lines 167 and 195) we intended these repetitions only to aid readability by reminding the reader of previously defined symbols; this has now been streamlined. Additionally, symbols such as $S_{a,\iota_{ik}}$, θ_i, θ_k, and γ_t were insufficiently introduced, as they originate from Valerio et al. (2026a), where the non-linear ACOPF-based CSS formulation is described in detail. We included explicit definitions in this manuscript: γ_t represents the curtailment of turbine t, $S_{a,\iota_{ik}}$ denotes the apparent power on edge a for conductor size ι, and θ denotes the voltage angle at nodes. The indices t_i and s_i are used within a unified formulation for node i, which may be associated with either turbines or a substation, rather than defining separate expressions for each node type.

3.1 Core formulation

Units of power are transferred through each edge and an integer variable $f_a \in \mathbb{Z}$ is associated with each candidate edge $a \in \mathcal{E}$, representing the number of turbine units transmitted between nodes i and k. Although the graph is undirected, each edge $a = (i, k)$ is assigned an arbitrary reference orientation for flow accounting purposes. A negative value of f_a therefore indicates flow opposite to the chosen orientation. The following constraint ensures that the power generated by all turbines is transmitted through the grid, and that no turbine remains unconnected:

$$p_i = \sum_{\substack{a=(i,k)\in\mathcal{E} \\ k\in\mathcal{N}_{ac},\, k\neq i}} f_a \qquad \forall i \in \mathcal{N}_{ac}. \tag{2}$$

- -

To limit the maximum number of turbines connected via a single string, the power flow on each edge is constrained such that

$$-\xi_a \cdot \mathfrak{M} \leq f_a \leq \xi_a \cdot \mathfrak{M}. \tag{5}$$

Here, $\mathfrak{M}$ is a parameter that represents the maximum allowable integer power flow per edge, equivalent to the maximum number of turbines per string,

....

3.2.1 Minimum turbines per string

This convention preserves the logic of Eq. (2), enabling the introduction of the following inequality constraint:

$$\xi_a \cdot \mathfrak{m} \leq f_a \leq \xi_a \cdot \mathfrak{M} \qquad \forall a \in \mathcal{E}_s. \tag{9}$$

Here, $\mathfrak{m}$ denotes the minimum turbine unit flow per string. To balance the number of turbines per string based on $\mathfrak{M}$, the minimum number of connections to the substations is determined from Eq.(7). Following this logic, $\mathfrak{m}$ can be calculated as...

- -

Non-Linear CSS

One possible formulation for cable size selection employs a non-linear model of AC power flow (ACOPF). This formulation considers the voltage magnitude V and angle θ at each node, and calculates the active P and reactive Q power flowing in each branch based on the branch admittance representation derived from $Y = G + jB$. The apparent power S_{ik} from node i to node k is then defined as

$$S_{ik} = P_{ik} + \mathrm{j}Q_{ik}, \tag{14a}$$
$$P_{ik} = |V_i|^2 G_{ff} + |V_i||V_k| \left[G_{ft}\cos(\theta_i - \theta_k) + B_{ft}\sin(\theta_i - \theta_k)\right], \tag{14b}$$
$$Q_{ik} = -|V_i|^2 B_{ff} + |V_i||V_k| \left[G_{ft}\sin(\theta_i - \theta_k) - B_{ft}\cos(\theta_i - \theta_k)\right]. \tag{14c}$$

Each node $i \in \mathcal{N}_{ac}$ is assumed to correspond to either a turbine or a substation, such that at most one of P_{t_i} or P_{s_i} is non-zero. Accordingly, the nodal power balance is given by

$$\gamma_{t_i} P_{t_i} - P_{s_i} = \sum_{\substack{k \in \mathcal{N}_{ac} \\ k \neq i}} P_{a_{\text{ik-eq}}} \qquad \forall i \in \mathcal{N}_{ac}, \tag{15a}$$
$$Q_{t_i} - Q_{s_i} = \sum_{\substack{k \in \mathcal{N}_{ac} \\ k \neq i}} Q_{a_{\text{ik-eq}}} \qquad \forall i \in \mathcal{N}_{ac}. \tag{15b}$$

Here, variables P_{t_i} and Q_{t_i} denote the active and reactive power generated at node i by a connected turbine, while P_{s_i} and Q_{s_i} represent the corresponding substation consumption. The term $\gamma_{t_i} P_{t_i}$ represents curtailed generation, where $\gamma_t = 1 - \text{curtailment}_{pu}$.

Reviewer's Concern 1.5

3. The distinction between non-linear and linear CSS (see Sections 4.1 and 4.2, respectively) is at best unclear. What non-linearities are in fact addressed in Section 4.1? Apparently, the only

non-linear relations that occur are products between one binary and one continuous variables, which by standard, simple techniques can be expressed in terms of linear inequalities (see inequalities (23)-(24)). The value of Section 4.1 seems dubious.

Authors' response 1.5
We acknowledge that the distinction between non-linear and linear CSS was not sufficiently clear. While products of binary and continuous variables can indeed be linearised using standard techniques (e.g. McCormick envelopes, as applied in our MILP CSS formulation), the non-linear ACOPF formulation involves additional non-linearities arising from power flow equations. In particular, the apparent power S is defined in terms of real and reactive power components, which depend non-linearly on voltage magnitudes and phase angles:

$$S_{ik} = P_{ik} + \mathrm{j}Q_{ik} \tag{4a}$$
$$P_{ik} = |V_i|^2 G_{ff} + |V_i||V_k| \left[G_{ft}\cos(\theta_i - \theta_k) + B_{ft}\sin(\theta_i - \theta_k)\right] \tag{4b}$$
$$Q_{ik} = -|V_i|^2 B_{ff} + |V_i||V_k| [G_{ft}\sin(\theta_i - \theta_k) - B_{ft}\cos(\theta_i - \theta_k) \tag{4c}$$

Here, S denotes apparent power, composed of real power P and reactive power Q; V is the voltage magnitude; and θ is the voltage angle at nodes i and k. The conductance G and susceptance B correspond to the real and imaginary parts of the admittance matrix $Y_{\text{bus-branch}}$. We revised Section 4.1 to clarify these distinctions and better justify its inclusion.

Non-Linear CSS
One possible formulation for cable size selection employs a non-linear model of AC power flow (ACOPF). This formulation considers the voltage magnitude V and angle θ at each node, and calculates the active P and reactive Q power flowing in each branch based on the branch admittance representation derived from $Y = G + jB$. The apparent power S_{ik} from node i to node k is then defined as

$$S_{ik} = P_{ik} + \mathrm{j}Q_{ik}, \tag{14a}$$
$$P_{ik} = |V_i|^2 G_{ff} + |V_i||V_k| \left[G_{ft}\cos(\theta_i - \theta_k) + B_{ft}\sin(\theta_i - \theta_k)\right], \tag{14b}$$
$$Q_{ik} = -|V_i|^2 B_{ff} + |V_i||V_k| \left[G_{ft}\sin(\theta_i - \theta_k) - B_{ft}\cos(\theta_i - \theta_k)\right]. \tag{14c}$$

Each node $i \in \mathcal{N}_{ac}$ is assumed to correspond to either a turbine or a substation, such that at most one of P_{t_i} or P_{s_i} is non-zero. Accordingly, the nodal power balance is given by

$$\gamma_{t_i} P_{t_i} - P_{s_i} = \sum_{\substack{k \in \mathcal{N}_{ac} \\ k \neq i}} P_{a_{\text{ik-eq}}} \qquad \forall i \in \mathcal{N}_{ac}, \tag{15a}$$
$$Q_{t_i} - Q_{s_i} = \sum_{\substack{k \in \mathcal{N}_{ac} \\ k \neq i}} Q_{a_{\text{ik-eq}}} \qquad \forall i \in \mathcal{N}_{ac}. \tag{15b}$$

Here, variables P_{t_i} and Q_{t_i} denote the active and reactive power generated at node i by a connected turbine, while P_{s_i} and Q_{s_i} represent the corresponding substation consumption. The term $\gamma_{t_i} P_{t_i}$ represents curtailed generation, where $\gamma_t = 1 - \text{curtailment}_{pu}$.

This allows the consideration of the trade-off between system losses and cable investment costs. Non-linear modelling captures the complete π model of cables, including inductance and, crucially for submarine cables, capacitance, which can increase reactive power and thereby lead to additional losses. The formulation of a non-linear CSS power flow is presented in (Valerio et al., 2026a), where each array section a includes multiple $Y_{\text{bus-branch}}$ elements corresponding to the various conductor types that may connect the node pair, as illustrated in Fig. 2.
The use of equivalent bus admittance matrices establishes a relationship in which the power at each end of the equivalent branch is determined by multiple binary factors $\xi_{a,\iota} \in \{0, 1\}$, which relate the apparent power flow associated with each conductor type, $S_{a,\iota}$, to the equivalent branch flows $S_{a_{\text{ik-eq}}}$ and $S_{a_{\text{ki-eq}}}$, such that

$$S_{a_{\text{ik-eq}}} = \sum_{\iota \in \mathcal{I}} \left(\xi_{a,\iota} \cdot S_{a,\iota_{\text{ik}}} \right), \tag{16a}$$

$$S_{a_{\text{ki-eq}}} = \sum_{\iota \in \mathcal{I}} \left(\xi_{a,\iota} \cdot S_{a,\iota_{\text{ki}}} \right). \tag{16b}$$

Here, $S_{a,\iota_{ik}}$ denotes the apparent power flow associated with conductor type ι on branch $a = (i, k)$, directed from node i to node k, where $\xi_{a,\iota}$ is indexed by both the branch position a and the conductor type $\iota \in \mathcal{I}$. The referenced paper presents a non-linear approach that considers internal system losses, allowing for the intentional over-sizing of conductor sections to reduce losses. These losses are incorporated into the main CSS objective within a multi-objective framework as follows:

$$\min \left[\frac{1 - (1 + r)^{-y}}{r} \cdot H_y \cdot \rho \cdot \left(\sum_{i \in \mathcal{N}_t} P_{t_i} - \sum_{i \in \mathcal{N}_s} P_{s_i} \right) \right]. \tag{17}$$

Here, the losses are calculated as the total power extracted by the substations, $\sum_{i \in \mathcal{N}_s} P_{s_i}$, minus the total power injected by the turbines, $\sum_{i \in \mathcal{N}_t} \gamma_{t_i} P_{t_i}$, in the array system. The economic parameter H_y denotes the full-load hours of system operation over y years, while ρ denotes the electricity cost, for example based on an assumed LCoE. The discount rate r enables a net present value (NPV) comparison with conductor investment costs. Both individual objectives are combined into a multi-objective function using a weighting parameter $\alpha \in \mathbb{R}_{\geq 0}$, which determines the relative importance of the loss-related term,

$$\min \left[(13) + \alpha (17) \right]. \tag{18}$$

2 Reviewer 2

Reviewer's Concern 2.1

The work addresses a relevant aspect of wind power plant optimization and offers a contribution regarding the inclusion of realistic details and constraints within the problem modeling and the optimization framework. The set of example cases presented as experiments employing the proposed method and its variants is valuable and illustrates some of the alternatives discussed.

That said, the manuscript is hard to follow. Symbol use precedes symbol definition in several cases. The manuscript would benefit from a structured symbol description summary early in the text. Moreover, the names for variables and procedures could be chosen so as to help the reader understand what they represent. A few specific examples are given in the detailed comments, but one that is used throughout the document is conflating "path-finding" with network design.

Reference Valerio et al. (2026b) is not published and seems essential to support part of the work presented in this manuscript. This reference seems to present one aspect that is missing from the manuscript: a comparison to the modeling choices and frameworks already described in the literature.

Detailed comments and technical corrections follow.

Authors' response 2.1

We appreciate the reviewer's detailed clarifications and have revised the manuscript accordingly.

Regarding symbol usage, the authors have added a list of symbols as Appendix A to aid readers requiring a reference table. In addition, the manuscript has undergone further proofreading, and the readability and presentation of variables have been improved following the comments from both reviewers.

Regarding comments [59] and [494], we agree that the contribution of the present work cannot be adequately assessed without access to the referenced manuscript.

Valerio et al. (2026b) is a conference paper accepted for publication at TORQUE 2026, which could have not been made publicly available until it was presented at the conference. For this reason, we contacted the editorial support team prior to the review process so that the non-public manuscript could have been made available to reviewers upon request. (https://doi.org/10.5194/wes-2026-53-AC1) As of now have been published and available online https://iopscience.iop.org/article/10.1088/1742-6596/3224/5/052005

The conference manuscript presents the graph preparation stage for offshore wind developments and the core MILP routing formulation, focusing on maximum turbines per string and maximum substation connections. These components are incorporated into the present WES manuscript and further extended as follows:

- Graph preparation: A distinction is introduced between offshore and onshore distances due to the offshore connection from the sea surface to the seabed, which depends on bathymetry. In addition, a distinction is made between weighted path length and conductor length for each path, differentiating the quantities used for routing and cable cost calculations.
- Routing algorithm: The core formulation is extended with additional user-defined strategies, including minimum turbines per string and unbalanced substation capacities.

Additionally, as referenced in comment [494], the conference manuscript presents a benchmark of the core MILP routing formulation against OptiWindNet from Souza de Alencar et al. (2025). The benchmark compares problem size in terms of the number of variables and constraints, as well

as solution time. The authors did not consider it appropriate to repeat these results in the WES manuscript, as the present work extends beyond the core MILP routing formulation by incorporating an independent conductor size selection methodology and, most importantly, a joint routing and conductor size optimisation framework, which cannot be directly benchmarked against OptiWindNet. As such, the case studies presented in the WES manuscript focus on comparing the two joint optimisation methodologies, namely the integrated and sequential approaches, as well as two additional case studies specific to the sequential framework with non-linear conductor size selection.

Reviewer's Concern 2.2

Abstract

[11-12] The abstract could mention the main outcomes of the evaluation of the approaches.

> ... Routing and conductor size selection may be combined within an integrated approach or implemented as a sequential algorithm to explore trade-offs between trenching and cabling costs. The proposed approaches are evaluated using current turbine ratings and the layouts of existing onshore and offshore projects. The integrated formulation generally achieves lower total costs, while the sequential approach offers greater modelling flexibility for constrained routing problems. The results further demonstrate that layouts with minimum trench length do not necessarily minimise total investment cost, since limiting the number of conductor types may exclude larger conductor capacities, thereby changing the feasible routing configurations and the conductor types ultimately selected within the system.

Reviewer's Concern 2.3

1 Introduction

[19-20] Prefer citing the original sources instead of citing works that just refer to the original sources.

[22] "Layout optimisation" in the context of wind power usually refers to choosing the positions of the wind turbines. Although it is technically correct to use "cable layout optimisation" for the inter-array cabling problem, using a more exclusive term such as "collection system" or "electrical network" or "internal grid" or "array cable routing" optimization would draw a clearer distinction between the disciplines.

[25-26] MST and TSP are not algorithms

[51-52] Sentence is missing a verb

[59] Reference Valerio et al. (2026b) is not published, but the current work builds on it. At least a pre-print should be made available to enable the assessment of the contributions of the current work.

[71] When you use "comprises", what follows should cover the entire solution, not only the first step. Maybe you meant "includes"?

Authors' response 2.3

Following the reviewers comments we have improved the introduction. Regarding comment [59] this has been address in concern 2.1.

1. Introduction
[19-20]....
Optimising this configuration is highly relevant for cost-effectiveness; for example, in bottom-fixed offshore wind farms, inter-array cables may account for up to approximately 8-9% of the levelised cost of energy (LCoE) (Serrano González et al., 2014; BGV Associates, 2025).

\- -

[22] & [25-26]....
To address collector system optimisation, various approaches have been employed, including graph-based methods derived from the minimum spanning tree (MST) and travelling salesman problem (TSP) formulations (Dutta and Overbye, 2012; Wei et al., 2017), ant colony optimisation (Taylor et al., 2023), mixed-integer linear programming (MILP) (Fischetti and Pisinger, 2018a,b; Pillai et al., 2015; Pérez-Rúa et al., 2020; Ulku and Alabas-Uslu, 2020; Souza de Alencar et al., 2025), and heuristic approaches (Cazzaro et al., 2020; El Mokhi and Addaim, 2020; Sedighi et al., 2018; Gong et al., 2018), including genetic algorithms (Moon et al., 2014; Wei et al., 2017; Smail et al., 2018) and particle swarm optimisation (Hou et al., 2016).

\- -

[51-52]....
In Pérez-Rúa et al. (2020), an integrated layout algorithm is proposed that can adapt to multiple substations and limit static crossings; however, when considering CSS, the method does not limit the number of permitted conductors. ...

\- -

[71]...
The final solution includes a graph preparation phase that incorporates exclusion zones and elevation into the identification of connections process (Section 2).

Reviewer's Concern 2.4
2 Graph Preparation

Is the time spent on graph preparation negligible?

[93-95] This description of the additional vertices would really benefit from a figure specifically illustrating the densification approach.

[106] Introduce what you mean by “every segment”, you were just talking about vertices in the previous sentence.

Authors' response 2.4

To follow up on the comments regarding Section 2, the answer depends on how “negligible” is defined. Considered independently, the graph preparation stage does increase the computational effort and runtime compared to directly creating a 2D distance matrix. To quantify this, Table A1 has been extended to include the graph generation times for the different optimisation case studies, which range from approximately one second to just under two minutes.

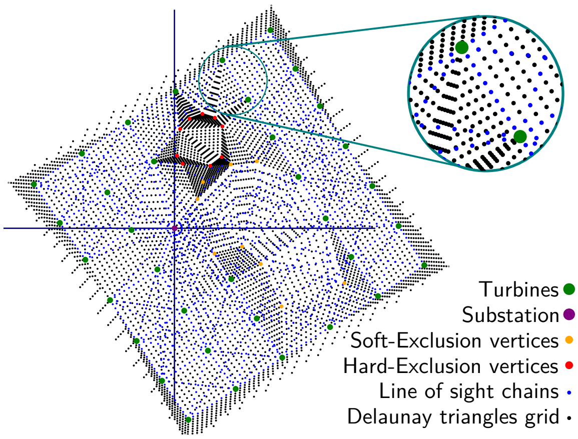

Figure 1: (b)

Several factors influence these runtimes. First, the complexity of the development area and the exclusion zones affects the triangulation of the area, resulting in a different number of densified points being added to the graph. Second, the graph preparation stage calculates A* connections from each substation to all turbines; therefore, case studies such as Hornsea 1 and Moray East, which contain multiple substations, require additional computational time.

For smaller case studies, such as Albatros and Alpha Ventus, the graph preparation stage can take a comparable amount of time to the optimisation itself. However, for larger systems, the graph preparation time may be considered negligible relative to the optimisation runtime.

For comments [93–95], we have improved Fig. 1(b) by adding colours to indicate the origin of each densified point, as well as a zoomed-in view to improve visibility.

Case Studies: Test systems for joint optimisation
Further case studies were implemented, covering wind parks ranging from 12 to 174 turbines, with power capacities between 2 and 14 MW, and including arrays with one to three substations. Detailed information of number of permissible edges, number of turbines, identified crossings, and turbine power and voltage is given in Table A1. The table also reports the graph preparation time for each case.

- -

2 Graph Preparation
[106] ..., as well as those outside the designated development area, are removed from the dataset, thereby also removing the segments connected to them. Two distinct quantities are associated with each remaining graph segment:

Reviewer's Concern 2.5
3 Minmum path connection

Reconsider the section title. The section seems to cover the minimization of the length of the entire network. "Path" is a simple sequence of nodes.

[134] "minimises the connections" sounds like an edge count minimization, but you are minimizing

total length or total weight (penalized length).

[136-137] Consider using “cycles” instead of “loops”, as the former is better aligned with graph terminology. “Cable strings” can also be improved by specifying that turbines can have a maximum degree of 2. Do you mean “simple path” instead of “single path”?

[139] Instead of “categorized”, use “partitioned” (more precise). Or state that $N_{ac} = (N_t \cup N_s)$.

[Eq. 5] Any particular reason to not use the simpler $|N_t|$ as the right-hand-side?

[161] Avoid symbol that is juxtaposition of two symbols (CP).

[215] spatially instead of “spacially”. If the development area is split in disjoint polygon, why not treat each as a separate problem?

[222] It is not clear what you mean by “which serves as a feasibility requirement rather than an optimisation constraint”. The optimization already includes many constraints that are connected to feasibility and that use user-specified parameters. What is different here?

Authors’ response 2.5

We acknowledge the section title could be improved. Following this suggestion, it has been modified to “Collector System Routing”. The remaining comments have been addressed directly in the manuscript.

Regarding comment [Eq. 5], the original formulation was developed considering Steiner nodes, such that:

$$\sum_{a \in \mathcal{E}} \xi_a \leq |\mathcal{N}_{ac}| - |\mathcal{N}_s|.$$

where $N_{ac} = N_t \cup N_s \cup N_{steiner}$ and $p_i = 0 \; \forall i \in N_{steiner}$. The current formulation is a simplified version of this original setup. However, without Steiner nodes, the right-hand side simplifies to $|N_t|$.

Regarding comment [215], if the development area is divided into disjoint polygons, these could potentially be treated as separate optimisation problems. However, this would also separate the subsequent conductor size selection stage and, more specifically, the routing constraints such as the maximum number of turbines per string. The formulation therefore retains this capability to provide flexibility when handling complex development zones.

Collector system routing

- -

[134]...
The second stage of the array optimisation process involves taking the undirected graph of feasible edges and selecting a configuration that minimises the connections total weight required to link all turbines to the substations.

- -

[136-137]...
A radial array is defined as a set of cable strings connecting turbines to substations without cycles. Each turbine lies on a simple path to a substation and may connect to at most two neighbouring turbines. The notation used in the minimum-route formulation is summarised in Table 1.

[139]...
The graph nodes ($\mathcal{N}_{ac}$) are initially partitioned into two sets: turbine nodes $\mathcal{N}_t \subseteq \mathcal{N}_{ac}$ and substation nodes $\mathcal{N}_s \subseteq \mathcal{N}_{ac}$, such that $\mathcal{N}_{ac} = \mathcal{N}_t \cup \mathcal{N}_s$. To maintain power flow tracking within the system, each turbine node injects one unit of power, modelled as a fixed parameter such that $p_i = 1$ for all $i \in \mathcal{N}_t$.

[Eq. 5]....

$$\sum_{a \in \mathcal{E}} \xi_a = |\mathcal{N}_t|. \tag{3}$$

[161]....
Furthermore, the binary variable enables the restriction of crossing pair activations, ensuring that at most one edge from each crossing pair is active. Crossing pairs are defined by the set $\mathcal{X}$ which denotes the set of unordered edge pairs (a, b) such that edges a and b geometrically intersect, as constrained by:

$$\xi_a + \xi_b \leq 1 \qquad \forall (a, b) \in \mathcal{X}. \tag{4}$$

[215]...
In certain projects, circumstances may necessitate the installation of substations with differing capacities, such as in spatially separated development areas.

[222]...
To accommodate differing capacities, it is required that the total installed capacity across all substations equals or exceeds the number of turbines, as specified in Eq. (12b), which acts as a consistency condition on the user-defined input parameters rather than a constraint involving optimisation variables, since substation capacities are fixed inputs and not subject to optimisation.

Reviewer's Concern 2.6

4 Conductor size selection

[230-231] Avoid creating mathematical symbols by simply concatenating letters (CT), it makes expressions harder to read. Does installation cost include acquisition cost? Is the latter not relevant?

[Eq.18] Discount rate is typically adimensional, so expression 17 has energy dimension and expression 15 has currency dimension. Why not bring both to a common dimension instead of introducing this abstract alpha parameter?

[Eq.20] γ_t is not defined

[Eq.25] This seems in conflict with the previous use of ξ. Shouldn't the right-hand-side be ξ_a? Or maybe you could formally define A_{ac}, given that "Aac is defined as the subset of E previously selected by a path algorithm" is not very precise.

[296] State what v_i is supposed to indicate.

Authors' response 2.6

The concerns have been addressed directly in the manuscript. Following Reviewer 1's comments, we have also expanded the explanation of the non-linear CSS formulation, which introduces several variables that were previously presented without sufficient explanation.

[230-231]...
For every connection between two nodes, a cable type ι must be selected from the mutually exclusive set $\mathcal{I}$, allowing only one conductor type per connection. ...
Each conductor type $\iota \in \mathcal{I}$ is characterised by a conductor cost per unit length ψ_ι. Accordingly, the objective function is defined as:

- -

[Eq.18].....

$$\min \left[\frac{1-(1+r)^{-y}}{r} \cdot H_y \cdot \rho \cdot \left(\sum_{i \in \mathcal{N}_t} P_{t_i} - \sum_{i \in \mathcal{N}_s} P_{s_i} \right) \right]. \tag{17}$$

Here, the losses are calculated as the total power extracted by the substations, $\sum_{i \in \mathcal{N}_s} P_{s_i}$, minus the total power injected by the turbines, $\sum_{i \in \mathcal{N}_t} \gamma_{t_i} P_{t_i}$, in the array system. The economic parameter H_y denotes the full-load hours of system operation over y years, while ρ denotes the electricity cost, for example based on an assumed LCoE.

- -

[Eq.20]...
Non-Linear CSS
One possible formulation for cable size selection employs a non-linear model of AC power flow (ACOPF). This formulation considers the voltage magnitude V and angle θ at each node, and calculates the active P and reactive Q power flowing in each branch based on the branch admittance representation derived from $Y = G + jB$. The apparent power S_{ik} from node i to node k is then defined as

$$S_{ik} = P_{ik} + \mathrm{j} Q_{ik}, \tag{14a}$$
$$P_{ik} = |V_i|^2 G_{ff} + |V_i||V_k| \left[G_{ft} \cos(\theta_i - \theta_k) + B_{ft} \sin(\theta_i - \theta_k) \right], \tag{14b}$$
$$Q_{ik} = -|V_i|^2 B_{ff} + |V_i||V_k| \left[G_{ft} \sin(\theta_i - \theta_k) - B_{ft} \cos(\theta_i - \theta_k) \right]. \tag{14c}$$

Each node $i \in \mathcal{N}_{ac}$ is assumed to correspond to either a turbine or a substation, such that at most one of P_{t_i} or P_{s_i} is non-zero. Accordingly, the nodal power balance is given by

$$\gamma_{t_i} P_{t_i} - P_{s_i} = \sum_{\substack{k \in \mathcal{N}_{ac} \\ k \neq i}} P_{a_{\text{ik}}\text{-eq}} \qquad \forall i \in \mathcal{N}_{ac}, \tag{15a}$$

$$Q_{t_i} - Q_{s_i} = \sum_{\substack{k \in \mathcal{N}_{ac} \\ k \neq i}} Q_{a_{\text{ik}}\text{-eq}} \qquad \forall i \in \mathcal{N}_{ac}. \tag{15b}$$

Here, variables P_{t_i} and Q_{t_i} denote the active and reactive power generated at node i by a connected turbine, while P_{s_i} and Q_{s_i} represent the corresponding substation consumption. The term $\gamma_{t_i} P_{t_i}$ represents curtailed generation, where $\gamma_t = 1 - \text{curtailment}_{pu}$. - - - -

- -

[Eq.25]....
In this section, the CSS problem is formulated assuming that the network routing has already been determined. Let $\mathcal{A} \subseteq \mathcal{E}$ denote the subset of active edges selected during the routing stage, such that $\xi_a = 1$ for all $a \in \mathcal{A}$....

- -

[296]...
To track which conductor types are used in the overall system and comply with criteria C5, the binary indicator $\nu_\iota \in \{0, 1\}$ is introduced. This indicator identifies whether conductor type ι is active within the system....

Reviewer's Concern 2.7

5 Joint routing and conductor size optimisation

[310] Feasibility is only determined by the maximum capacity cable type available. In terms of feasibility, the CSS and routing problems are decoupled.

[331] Isn't the number of active branches at least the same as the number of turbines?

[350] When you say it does not increase linearly, is the relationship superlinear or sublinear? How does the conclusion follow from the premise?

[360] It seems like the first formal definition of A_{ac} is in fig.3. This definition would be useful much earlier in the manuscript. It seems like a poor naming choice to call it "permissible edges". Isn't A_{ac} the set of active edges of a routing solution?

[Fig.3] Maybe unifying "initialize CT" and "CT <- $\{\ldots\}$" at the top of the diagram would make it clearer what the loop is actually iterating over.

Authors' response 2.7

Following the comment on [310], "feasibility" was not the appropriate term to use in this context, and the wording has been improved accordingly.

Regarding comment [331], this issue was not only related to the previous comment on [Eq. 5] (now Eq. 3), but also resulted from a typo. For the present work, the formulation has been simplified to $|N_t|$.

For comment [350], the cable cost function from (Dicorato et al., 2011) is used, in which a

linear relationship between cross-sectional area and cost is assumed. However, there is no linear relationship between cable capacity and cross-sectional area, as illustrated in Fig. R1 it shows a sublinear relationship. Information regarding this relationship has been added in the new Appendix C.

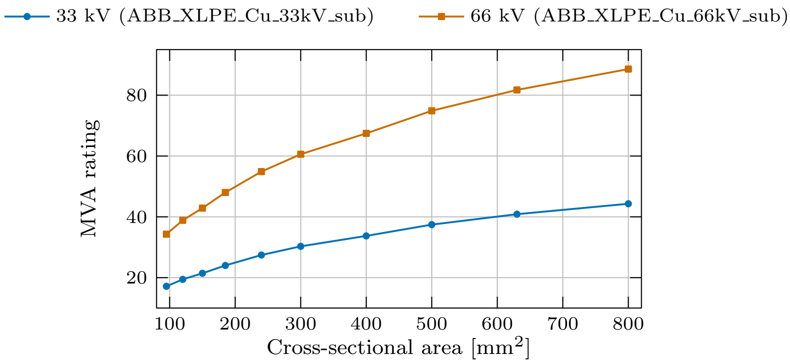

Figure R1: Cross-sectional area to power rating

The comment on [Fig. 3] has been addressed by replacing "Initialize $\mathcal{CT}$" with "$\mathcal{I} \leftarrow \mathcal{I}_{\text{all}}$".

[310]..
In Section 4, conductor size selection was formulated assuming that the routing of the array system was already determined. Under this formulation, cable diameters are assigned to a fixed network topology. However, the routing configuration and conductor sizing are inherently coupled, since limiting the set of conductor types also limits the maximum transferable power within the network. Importantly, this limit is determined not by the largest conductor type available overall, but by the largest conductor type selected for use in the network.

- -

[331]...
the term ($|\mathcal{N}_t|$) provides an upper bound on the number of branches. Accordingly, Eq. (26a) is reformulated as follows:

$$\sum_{a \in \mathcal{E}} \xi_{a,\iota} - |\mathcal{N}_t| \cdot \nu_\iota \leq 0 \qquad \forall \iota \in \mathcal{I}. \tag{29}$$

- -

[360]...
4 Conductor Size selection
In this section, the CSS problem is formulated assuming that the network routing has already been determined. Let $\mathcal{A} \subseteq \mathcal{E}$ denote the subset of active edges selected during the routing stage, such that $\xi_a = 1$ for all $a \in \mathcal{A}$.
5.2 Sequential Algorithm

The resulting subset of edges determined by the routing optimisation, $\mathcal{A}$, is then evaluated using either a non-linear CSS approach...

Reviewer's Concern 2.8

6 Layout modelling

[397] By "those obtained without bifurcations" do you mean those obtained with bifurcations? You should show some evidence (empirical or theoretical) that radial configurations help in approaching optimality.

[Table 1] The "Type" column should use some short handle that helps to understand the different methods. Using subsection numbers is too obscure.

[405] The linear costs used for each cable type should be presented as a table.

[420-425] What is the voltage level used for that example?

[436] Hornsea 1 has 174 turbines.

[439] Please clarify "pathfinding mechanism can identify hook-shaped strings to optimise interconnections"

[470] The role of the use of the assumed LCoE in the comparison is not clear. What was the value for alpha used in those non-linear examples?

[Table 5] How are the costs associated with losses computed?

Authors' response 2.8

The concerns have been addressed directly in the manuscript. Regarding the statement "pathfinding mechanism can identify hook-shaped strings to optimise interconnections", we have improved the wording to better reflect the intended meaning, namely routing configurations where the power flow path initially extends away from the substation geographically before returning to connect additional turbines. This was intended to highlight the flexibility of the undirected graph approach.

[397] ....
Since radial configurations are a subset of radial-star configurations, the resulting layouts cannot be shorter than those obtained with bifurcations; however, the reduced solution space can aid the solver in approaching optimality.

- -

[405] & [420-425]...
6 Case Studies
... The data associated with the case studies, including array voltage, turbine rated power, and graph creation results from Section 2, such as the number of nodes, edges, crossings, and graph generation time, is presented in Appendix B, while the conductor type data is presented in Appendix C.

- -

[436]...
HornSea I [GB-ENG] (Fig. 7(a),7(b) serves as the largest test case, with 174 turbines and

three substations.

– –

[439]...
... *Horn Rev 2 [DK]* (Fig. 7(e),7(f)) illustrates how the routing mechanism can identify non-direct string layouts to optimise interconnections....

– –

[470] & [Table 5]...
4.1 Non linear CSS These losses are incorporated into the main CSS objective within a multi-objective framework as follows:

$$\min \left[\frac{1-(1+r)^{-y}}{r} \cdot H_y \cdot \rho \cdot \left(\sum_{i \in \mathcal{N}_t} P_{t_i} - \sum_{i \in \mathcal{N}_s} P_{s_i} \right) \right]. \tag{17}$$

Here, the losses are calculated as the total power extracted by the substations, $\sum_{i \in \mathcal{N}_s} P_{s_i}$, minus the total power injected by the turbines, $\sum_{i \in \mathcal{N}_t} \gamma_{t_i} P_{t_i}$, in the array system. The economic parameter H_y denotes the full-load hours of system operation over y years, while ρ denotes the electricity cost, for example based on an assumed LCoE. The discount rate r enables a net present value (NPV) comparison with conductor investment costs. Both individual objectives are combined into a multi-objective function using a weighting parameter $\alpha \in \mathbb{R}_{\geq 0}$, which determines the relative importance of the loss-related term:

$$\min \left[(13) + \alpha (17) \right]. \tag{18}$$

6.3 Comparison with Non-linear CSS approach
... To enable a direct comparison between losses and investment costs, the value of α in (18) is set to 1. ...
... For a comparable assessment, losses are also calculated using a Newton–Raphson power flow applied to the grids obtained from the linear approaches. These results are presented in Table 7. ....

Reviewer's Concern 2.9
7 Discussion

[491] Again, a reference to the unavailable work with great relevance for the assessment of the current work.

[494] Using the time to "last feasible solution" as a reference seems odd. Either you reference the first feasible solution (i.e. time to feasibility) or you use the gap (time to a reach a pre-defined gap).

Authors' response 2.9

Regarding comment [491], this concern has been addressed in Section 2.1. The time to feasibility can strongly depend on the solver settings selected by the user. For example, in Gurobi, the optimisation can be configured to prioritise gap reduction or the rapid identification of an initial feasible

solution. In the presented case studies, finding the first feasible solution was generally not the most computationally demanding stage. Instead, due to the large number of crossing constraints, reducing the optimality gap represented the main computational challenge. The paragraph has therefore been reworded to better convey this discussion.

[494]...
Shifting focus to full-park optimisation with CSS, as presented in Section 6.2, the integrated results reveal that in most cases the optimisation reaches the imposed time limit. However, feasible solutions are typically identified within a relatively short time window, after which the optimisation primarily focuses on reducing the optimality gap. Although the gap generally decreases over time, convergence can be slow, making it difficult to prove optimality within practical computational limits. Consequently, selecting an appropriate cut-off time that balances computational effort and solution quality remains non-trivial. For example, in the case of *Griffin [GB-SCT]*, the last feasible solution is found very close to the time limit.

A List of symbols

A.1 Sets and indices

$\mathcal{N}_{ac}$	Set of all nodes in the network
$\mathcal{N}_t$	Set of turbine nodes
$\mathcal{N}_s$	Set of substation nodes
$\mathcal{E}$	Set of candidate edges
$\mathcal{E}_i$	Set of edges connected to node i
$\mathcal{A}$	Set of active edges selected by the routing stage
$\mathcal{I}$	Set of available conductor types
i, k	Indices of network nodes
$a = (i, k)$	Edge connecting nodes i and k
ι	Index of conductor type
$\mathcal{F}$	Feasible solution set

A.2 Decision variables

ξ_a	Binary variable indicating whether edge a is active
$\xi_{a,\iota}$	Binary variable indicating assignment of conductor type ι to edge a
ν_ι	Binary variable indicating whether conductor type ι is used
f_a	Integer power flow on edge a
$z_{a,\iota}$	Auxiliary variable for McCormick linearisation
$\iota_{\max}^{(i)}$	Largest conductor type that was assigned

A.3 Routing design parameters

p_i	Net power injection at node i
$\mathfrak{M}$	Maximum number of turbines per string
$\mathfrak{m}$	Minimum number of turbines per string
$\mathfrak{s}_s$	Minimum number of string connections per substation
$\mathfrak{S}_s$	Maximum number of connections per substation
$\mathfrak{M}_\iota$	Flow capacity of conductor type ι
$\mathfrak{N}$	Maximum number of conductor types allowed
$\mathcal{W}_a$	Weighted length of edge a
L_a	Geometric length of edge a
ψ_a	Installation cost per unit weighted length
ψ_ι	Cost per unit length of conductor type ι

A.4 Electrical quantities

V_i	Voltage magnitude at node i
θ_i	Voltage angle at node i
P_{ik}, Q_{ik}	Active and reactive power flow from node i to node k
S_{ik}	Apparent power flow from node i to node k
$S_{a,\iota_{ik}}$	Apparent power flow on branch a using conductor type ι

P_{t_i}, Q_{t_i}	Active and reactive turbine power at node i
P_{s_i}, Q_{s_i}	Active and reactive substation power at node i
γ_{t_i}	Curtailment factor at turbine node i
M_a	Big-M parameter for branch a
κ	Security factor for M_a

A.5 Economic parameters

α	Weighting parameter in the multi-objective function
r	Discount rate
y	Project lifetime (years)
H_y	Full-load hours over y years
ρ	Electricity cost

B Case Information

This appendix provides detailed information on the test cases and their corresponding results. Table I summarises the specific characteristics of each case.

C Conductor dataset

This appendix provides information on the conductor sets used in the test cases. The cable data are compiled from (ABB, 2010a) for onshore cables and (ABB, 2010b) for offshore submarine cables. In all simulations, the cost per metre of each conductor is estimated as

$$\text{Cost} = 0.4818 \cdot S + 99.153 \quad [\text{k€ km}^{-1}], \tag{10}$$

taken from Dicorato et al. (2011), where S denotes the conductor cross-sectional area. In this approximation, neither the voltage level nor the conductor material is explicitly considered. Consequently, the resulting cost values are employed solely for methodology validation within the presented case studies and should not be interpreted as industrial quotations, project-specific estimates, or commercially validated cable prices.

For onshore 33 kV cables in Table II, reference (ABB, 2010a) does not provide data directly; therefore, the corresponding values were extrapolated from the available voltage levels. For the conductors used in the Non-linear CSS in Table VII, the cable parameters are taken from the ABB dataset, whereas the cable capacities are taken from (Marine Scotland, 2019, 2020).

Table I: Cases detailed information

Case	Turbine	Array	Graph			
	Power [MW]	Voltage [kV]	Nodes	Edges	Crossings	Time [s]
Albatros [DE]	7	33	17	67	150	3.08
Alpha ventus [DE]	5	66	13	48	93	1.37
Anholt [DK]	3.6	33	112	514	1853	25.32
Arcadis Ost [DE]	9.5	66	28	120	357	8.61
Baltic eagle [DE]	9.5	66	51	270	1113	8.93
Barrow [GB-ENG]	3	33	31	150	643	5.87
Beatrice [GB-SCT]	7	33	86	506	5111	28.66
DanTysk [DE]	3.6	33	81	386	2152	20.74
Fryslaan [NL]	4.3	33	90	528	2964	17.14
Global Tech I [DE]	5	33	81	443	1764	16.66
HornSea I [GB-ENG]	7	33	177	1144	32700	115.54
HornSea II [GB-ENG]	8	66	166	859	4869	46.87
HornsRev 1 [DK]	2	33	81	470	2469	15.68
HornsRev 2 [DK]	2.3	33	92	488	2440	15.06
HornsRev 3 [DK]	8	33	50	254	770	10.12
Kaskasi [DE]	8	66	39	184	666	5.14
Kentish [GB-ENG]	3	33	44	230	905	7.98
Meerwind Sud Ost [DE]	3.6	33	81	418	1818	12.77
Moray East [GB-SCT]	9.5	66	103	619	13429	47.19
Moray West [GB-SCT]	14	66	62	330	2523	20.66
Nordsee One [DE]	6.2	33	55	274	1022	9.65
Nordsee Ost [DE]	6.2	66	43	205	576	7.28
Princess amalia [NL]	2	22	61	328	1124	9.70
Seagreen [GB-SCT]	10	66	115	634	3213	28.39
Thanet [GB-ENG]	3	33	101	571	2803	16.07
Triton Knoll [GB-ENG]	9.5	66	92	515	6257	21.92
West of Duddon [GB-ENG]	3.6	33	109	599	2627	17.77
Westermost Rough [GB-ENG]	6	33	36	154	410	9.55
Bhlaraidh [GB-SCT]	3.45	33	34	167	693	15.69
Bronco Plains [US]	2.8	33	107	617	3079	20.06
Coromuel [MX]	2.8	33	21	55	190	8.86
Griffin [GB-SCT]	2.3	33	69	336	2275	12.80
Serra Voltorera [ES]	1.67	33	11	38	256	1.27
Storheia vindpark [NO]	3.6	33	81	428	3203	48.71
Stronelairg [NO]	3.45	33	64	504	1115	16.75
Trucafort one [ES]	0.225	33	66	313	2649	8.58
Trucafort two [ES]	0.6	33	26	88	306	3.04

Table II: ABB XLPE Cu 33 kV ground trefoil cable parameters

Cross-sectional area(S) [mm^2]	Capacitance [μF km^{-1}]	Power capacity [MVA]	Cost [€ km^{-1}]
95	0.191	13.146	144,924
120	0.196	14.932	156,969
150	0.224	16.719	171,423
185	0.234	18.862	188,286
240	0.258	22.006	214,785
300	0.278	24.721	243,693
400	0.313	28.364	291,873
500	0.347	32.223	340,053
630	0.377	36.581	402,687
800	0.407	41.225	484,593
1000	0.452	45.583	580,953
1200	0.517	48.941	677,313
1400	0.551	51.871	773,673
1600	0.581	54.228	870,033
2000	0.626	58.301	1,062,753

Table III: ABB XLPE Cu 66 kV ground trefoil cable parameters

Cross-sectional area(S) [mm^2]	Capacitance [μF km^{-1}]	Power capacity [MVA]	Cost [€ km^{-1}]
95	0.160	26.293	144,924
120	0.180	29.865	156,969
150	0.190	33.437	171,423
185	0.200	37.724	188,286
240	0.220	44.011	214,785
300	0.240	49.441	243,693
400	0.260	56.729	291,873
500	0.290	64.445	340,053
630	0.320	73.162	402,687
800	0.350	82.450	484,593
1000	0.380	91.166	580,953
1200	0.430	97.883	677,313
1400	0.460	103.741	773,673
1600	0.490	108.457	870,033
2000	0.520	116.602	1,062,753

Table IV: ABB XLPE Cu 20 kV submarine cable parameters

Cross-sectional area(S) [mm^2]	Capacitance [μF km^{-1}]	Power capacity [MVA]	Cost [€ km^{-1}]
95	0.230	10.392	144,924
120	0.250	11.778	156,969
150	0.270	12.990	171,423
185	0.290	14.549	188,286
240	0.320	16.628	214,785
300	0.350	18.360	243,693
400	0.390	20.438	291,873
500	0.430	22.690	340,053
630	0.480	24.768	402,687

Table V: ABB XLPE Cu 33 kV submarine cable parameters

Cross-sectional area(S) [mm^2]	Capacitance [μF km^{-1}]	Power capacity [MVA]	Cost [€ km^{-1}]
95	0.180	17.147	144,924
120	0.190	19.434	156,969
150	0.210	21.434	171,423
185	0.220	24.006	188,286
240	0.240	27.436	214,785
300	0.260	30.294	243,693
400	0.290	33.723	291,873
500	0.320	37.438	340,053
630	0.350	40.868	402,687
800	0.380	44.297	484,593

Table VI: ABB XLPE Cu 66 kV submarine cable parameters

Cross-sectional area(S) [mm^2]	Capacitance [μF km^{-1}]	Power capacity [MVA]	Cost [€ km^{-1}]
95	0.170	34.295	144,924
120	0.180	38.867	156,969
150	0.190	42.868	171,423
185	0.200	48.012	188,286
240	0.220	54.871	214,785
300	0.240	60.587	243,693
400	0.260	67.446	291,873
500	0.290	74.877	340,053
630	0.320	81.735	402,687
800	0.350	88.594	484,593
1000	0.380	94.310	580,953

Table VII: ABB XLPE Al 66 kV submarine cable parameters

Cross-sectional area(S) [mm^2]	Resistance [$\Omega\,km^{-1}$]	Inductance [$mH\,km^{-1}$]	Capacitance [$\mu F\,km^{-1}$]	Power capacity [MVA]	Cost Cost [€ km^{-1}]
240	0.151	0.380	0.220	40.0	214,785
300	0.121	0.370	0.240	54.0	243,693
630	0.060	0.330	0.320	80.0	402,687
800	0.049	0.320	0.350	84.2	484,593

References

ABB: XLPE Land Cable Systems: User's Guide, ABB, rev. 5 edn., 2010a.

ABB: XLPE Submarine Cable Systems: Attachment to XLPE Land Cable Systems - User's Guide, ABB, rev. 5 edn., https://new.abb.com/docs/default-source/ewea-doc/xlpe-submarine-cable-systems-2gm5007.pdf, 2010b.

BGV Associates: Wind Farm Costs, https://guidetoanoffshorewindfarm.com/wind-farm-costs/, 2025.

Cazzaro, D., Fischetti, M., and Fischetti, M.: Heuristic algorithms for the Wind Farm Cable Routing problem, Applied Energy, 278, 115 617, https://doi.org/10.1016/j.apenergy.2020.115617, 2020.

Dicorato, M., Forte, G., Pisani, M., and Trovato, M.: Guidelines for assessment of investment cost for offshore wind generation, Renewable Energy, 36, 2043–2051, https://doi.org/10.1016/j.renene.2011.01.003, 2011.

Dutta, S. and Overbye, T. J.: Optimal Wind Farm Collector System Topology Design Considering Total Trenching Length, IEEE Transactions on Sustainable Energy, 3, 339–348, https://doi.org/10.1109/TSTE.2012.2185817, 2012.

El Mokhi, C. and Addaim, A.: Optimal Substation Location Of A Wind Farm Using Different Metaheuristic Algorithms, in: 2020 IEEE 6th International Conference on Optimization and Applications (ICOA), pp. 1–6, https://doi.org/10.1109/ICOA49421.2020.9094469, 2020.

Fischetti, M. and Pisinger, D.: Optimizing wind farm cable routing considering power losses, European Journal of Operational Research, 270, 917–930, https://doi.org/10.1016/j.ejor.2017.07.061, 2018a.

Fischetti, M. and Pisinger, D.: Optimal wind farm cable routing: Modeling branches and offshore transformer modules, Networks, 72, 42–59, https://doi.org/10.1002/net.21804, 2018b.

Gong, X., Kuenzel, S., and Pal, B. C.: Optimal Wind Farm Cabling, IEEE Transactions on Sustainable Energy, 9, 1126–1136, https://doi.org/10.1109/TSTE.2017.2771147, 2018.

Hou, P., Hu, W., Chen, C., and Chen, Z.: Overall Optimization for Offshore Wind Farm Electrical System, Wind Energy, 20, https://doi.org/10.1002/we.2077, 2016.

Marine Scotland: Moray East Offshore Wind Farm Cable Plan, Tech. rep., Marine Scotland, https://marine.gov.scot/sites/default/files/owf_cable_plan_v2_final_redacted.pdf, 2019.

Marine Scotland: Moray West Offshore Wind Farm Cable Plan, Tech. rep., Marine Scotland, https://marine.gov.scot/sites/default/files/846005-dbha10-mww-pln-000001_moray_west_wind_farm_cable_plan_rev01.pdf, 2020.

Moon, W.-S., Kim, J.-C., Jo, A., and Won, J.-N.: Grid optimization for offshore wind farm layout and substation location, in: 2014 IEEE Conference and Expo Transportation Electrification Asia-Pacific (ITEC Asia-Pacific), pp. 1–6, https://doi.org/10.1109/ITEC-AP.2014.6941124, 2014.

Pillai, A., Chick, J., Johanning, L., Khorasanchi, M., and de Laleu, V.: Offshore wind farm electrical cable layout optimization, Engineering Optimization, 47, 1689–1708, https://doi.org/10.1080/0305215X.2014.992892, 2015.

Pérez-Rúa, J.-A., Stolpe, M., and Cutululis, N. A.: Integrated Global Optimization Model for Electrical Cables in Offshore Wind Farms, IEEE Transactions on Sustainable Energy, 11, 1965–1974, https://doi.org/10.1109/TSTE.2019.2948118, 2020.

Sedighi, M., Moradzadeh, M., Kukrer, O., and Fahrioglu, M.: Simultaneous optimization of electrical interconnection configuration and cable sizing in offshore wind farms, Journal of Modern Power Systems and Clean Energy, 6, 749–762, https://doi.org/10.1007/s40565-017-0366-0, 2018.

Serrano González, J., Burgos Payán, M., Santos, J. M. R., and González-Longatt, F.: A review and recent developments in the optimal wind-turbine micro-siting problem, Renewable and Sustainable Energy Reviews, 30, 133–144, https://doi.org/https://doi.org/10.1016/j.rser.2013.09.027, 2014.

Smail, H., Alkama, R., and Medjdoub, A.: Optimal design of the electric connection of a wind farm, Energy, 165, 972–983, https://doi.org/10.1016/j.energy.2018.10.015, 2018.

Souza de Alencar, M., Göçmen, T., and Cutululis, N. A.: Flexible cable routing framework for wind farm collection system optimization, European Journal of Operational Research, https://doi.org/10.1016/j.ejor.2025.07.069, 2025.

Taylor, P., Yue, H., Campos-Gaona, D., Anaya-Lara, O., and Jia, C.: Wind farm array cable layout optimisation for complex offshore sites—A decomposition based heuristic approach, IET Renewable Power Generation, 17, 243–259, https://doi.org/https://doi.org/10.1049/rpg2.12593, 2023.

Ulku, I. and Alabas-Uslu, C.: Optimization of cable layout designs for large offshore wind farms, International Journal of Energy Research, 44, 6297–6312, https://doi.org/10.1002/er.5336, 2020.

Valerio, B. C., Cheah-Mane, M., Lacerda, V. A., Gebraad, P., and Gomis-Bellmunt, O.: Transmission expansion planning for hybrid AC/DC grids using a mixed-integer non-linear programming approach, International Journal of Electrical Power & Energy Systems, 174, 111 459, https://doi.org/https://doi.org/10.1016/j.ijepes.2025.111459, 2026a.

Valerio, B. C., Gebraad, P. M., Cheah-Mane, M., Lacerda, V., and Gomis-Bellmunt, O.: Strategies for wind park inter array optimisation through Mixed Integer Linear Programming, Journal of Physics: Conference Series, 3224, 052 005, https://doi.org/10.1088/1742-6596/3224/5/052005, 2026b.

Wei, S., Zhang, L., Xu, Y., Fu, Y., and Li, F.: Hierarchical Optimization for the Double-Sided Ring Structure of the Collector System Planning of Large Offshore Wind Farms, IEEE Transactions on Sustainable Energy, 8, 1029–1039, https://doi.org/10.1109/TSTE.2016.2646061, 2017.